Bayesian Tomography of Soft X-ray and Bolometer systems using Gaussian Processes

D. Li[1], J.Svensson[1], H.Thomsen[1], F.Medina[2], D.H. Zhang[1], T. Stange, A. Werner[1], R. Wolf[1]
[1] *Max Planck Institute for Plasma Physics, Teilinstitut D-17491 Greifswald,Germany*
[2] *Asociación EURATOM-CIEMAT, Madrid, Spain*

1. Introduction

A new Bayesian tomographic method for soft x-ray and bolometer diagnostic systems has been developed. The method is non-parametric in the sense of using Gaussian processes to model the underlying emissivity distribution, and the regularization of such a model becomes defined by a multivariate normal distribution at the points where the emissivity distributions should be evaluated [1,2]. As opposed to currently used other methods, e.g. Maximum entropy [3] (MaxEnt) and Equilibrium-Based Iterative Tomography Algorithm [4] (EBITA), to which this method is compared, this method is fully analytical, involving no nonlinear iterations, and so can be feasible for real-time applications. Additionally, uncertainties of the solution, accounting for both measurement uncertainties and ambiguities due to insufficient coverage of sight lines, can be provided by direct sampling from the posterior probability distribution. Describing the emissivity distribution by Gaussian processes [5,6] has the further advantage that regularization can be expressed in a natural way as correlation length scales of a diffusion process. In particular, the method can locally adapt the length scales to the varying smoothness of the emissivity distribution. This method has been applied to three different experiments: soft x-ray reconstructions for the W7-AS and TJ-II stellarators, and bolometer reconstructions for the WEGA stellarator, comparing favourably to currently used methods.

2. Method

In nuclear fusion, a conventional way to observe the plasma is the line integral measurement across a target region of the plasma by a detector located outside the plasma region. By using multiple detector arrays, a soft x-ray diagnostic system can spatially resolve emissivity distributions with a very high time resolution. In a similar way, a bolometer system can infer the distribution of total radiated power. The emissivity/radiation distributions over a 2D poloidal cross section can be expressed as $f(\bar{r})$ and a line-integrated signal is obtained from

$$d_l = c_l \cdot \int_{S_l} ds \cdot f(\bar{r}) + \varepsilon_l, \quad l = 1, 2, \ldots, M \tag{1}$$

where, the integral along line of sight path S_l is carried out within the solid angle subtended by one of M available detectors. The calibration factors c_l relates to the slight differences in spectral efficiencies and solid angles between the detectors. ε_l denotes an error term including both random and systematic uncertainties suffered by the diagnostic system.

In this Bayesian method, the posterior probability $p(\overline{f}_N|\overline{d}_M,\overline{\theta})$ over all possible solutions is deduced from the product of a prior $p(\overline{f}_N|\overline{\theta})$ and a likelihood $p(\overline{d}_M|\overline{f}_N,\overline{\theta})$, divided by an evidence term $p(\overline{d}_M|\overline{\theta})$ (marginal likelihood of data with respect to model assumptions):

$$p(\overline{f}_N|\overline{d}_M,\overline{\theta}) = \frac{p(\overline{d}_M|\overline{f}_N,\overline{\theta})\cdot p(\overline{f}_N|\overline{\theta})}{p(\overline{d}_M|\overline{\theta})} \quad (2)$$

where, the prior acts as a regularization on $\overline{f}_N$ to express our knowledge of it before any measurement; the likelihood introduces the constraints from the measured data within required data fits, finally the evidence term relates directly to the prior model assumptions, and can be used to optimize the model hyper-parameters $\overline{\theta}$. In this tomographic method [1], a Gaussian Process [5,6], is applied to construct the prior as a multivariate normal distribution:

$$p\left(\overline{f}_N\middle|\overline{\theta}\right)=\frac{1}{(2\pi)^{N/2}\left|\overline{\overline{\Sigma}}_f\right|^{1/2}}\exp\left[-\frac{1}{2}\left(\overline{f}_N-\overline{m}_f\right)^T\overline{\overline{\Sigma}}_f^{-1}\left(\overline{f}_N-\overline{m}_f\right)\right] \quad (3)$$

where here $\overline{\overline{\Sigma}}_f$ is calculated from the so called squared exponential covariance function, defining the covariance between two points $\overline{r}_i$, $\overline{r}_j$:

$$k_{SE}\left(\overline{r}_i,\overline{r}_j\right)=\sigma_f^2\exp\left(-\frac{d_{ij}^2}{2l^2}\right),\quad d_{ij}=\left\|\overline{r}_i-\overline{r}_j\right\| \quad (4)$$

where (σ_f, l) are the hyper-parameters $\overline{\theta}$, determining the properties of the random process, in this case the overall magnitude of the emission (σ_f), and a length scale l. These hyper-parameters can be determined by maximizing the evidence term in Eq.(2) in the space of $\overline{\theta}$. For further details of this method see [1] or [2]. The posterior distribution evaluated at a number of discrete points in the simulated emissivity region, will be a multivariate normal distribution with mean and covariance given by

$$\overline{m}_f^{post}=\overline{m}_f+\left(\overline{\overline{R}}^T\overline{\overline{\Sigma}}_d^{-1}\overline{\overline{R}}+\overline{\overline{\Sigma}}_f^{-1}\right)^{-1}\overline{\overline{R}}^T\overline{\overline{\Sigma}}_d^{-1}\left(\overline{d}_M-\overline{\overline{R}}\,\overline{m}_f\right) \quad (5)$$

$$\overline{\overline{\Sigma}}_f^{post}=\left(\overline{\overline{R}}^T\overline{\overline{\Sigma}}_d^{-1}\overline{\overline{R}}+\overline{\overline{\Sigma}}_f^{-1}\right) \quad (6)$$

Eq.(5) will give a single most likely reconstruction and Eq.(6) will give the uncertainty of the reconstruction. Uncertainties of functions of the distribution (such as total power) can be calculated by repeated sampling from the multivariate normal distribution with (5) as mean and (6) as covariance matrix, and forming a histogram of the function values calculated from each sample.

3. Performances and Results

3.1 Application to the soft X-ray system at the W7-AS stellarator.

In W7-AS, the dependence of the maximum achievable thermal/magnetic pressure ratio β on the equilibrium magnetic flux surface has been extensively investigated [7]. Since the emission relevant parameters e.g. plasma density, temperature are expected to be approximately constant within the equilibrium flux surfaces calculated by the Variational Moments Equilibrium Code [8] (VMEC), the basic features of the reconstructed emissivity distribution should approximately agree with the equilibrium flux, hence the β induced effects on equilibrium flux surfaces can be investigated by tomographic analysis. The reconstructions by this method in Fig.1(b) shows a strong outward shift due to high β, and structures consistent with VMEC equilibrium analysis, with the exception of a large indentation in the inboard side, which may arise from an increased peaking of the pressure profile in the plasma center. Fig.1(c) shows reconstructions of an m=3 mode structure which distributes symmetrically around the axis of the flux surface.

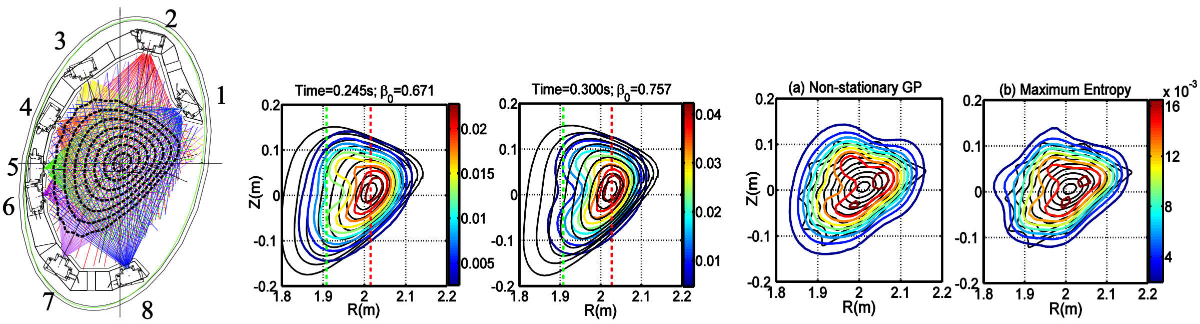

(a) (b) (c)

Fig.1: (a) A schematic view of the miniature soft X-ray system (MiniSoX diagnostic system) in W7-AS with eight compact detector arrays having a total of 256 sight lines. (b) Reconstructions by this (left) and MaxEnt (right) methods in high β performance. The green and red lines indicate the locations of the magnetic axis of the vacuum and finite β configurations, respectively. (c) Reconstructions by two methods with mode structures.

3.2 Application to the bolometer systems at WEGA and TJ-II stellarators

WEGA is a five period stellarator with a major radius of 0.72m and the coverage of 16 lines of sight from the bolometer system is shown in Fig.2(a). When the plasma axis is at $R = 702mm$, the center of reconstruction (Fig.2 (b)) has a consistent location. In a different pulse when the plasma axis is shifted to $R = 720mm$, the center of reconstruction (Fig.2 (c)) moves to the same location. For both pulses an OXB heating (with a deposition region $r \approx 10mm$) is applied, the reconstructions also coincide with the localized feature of such a heating approach.

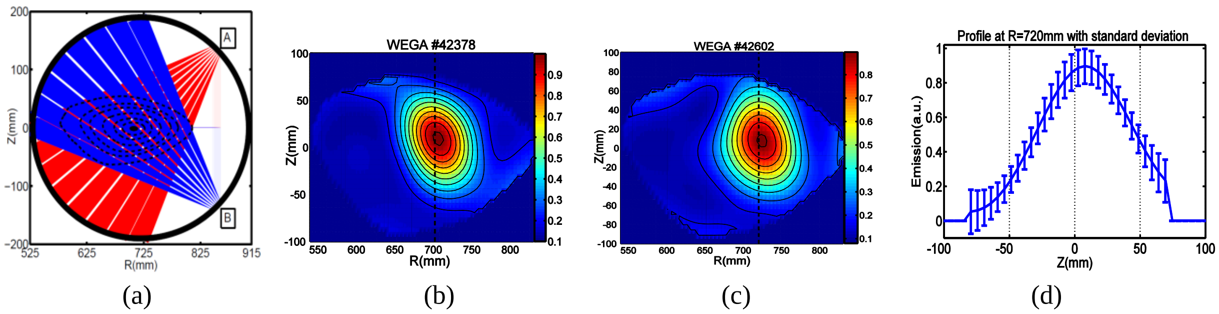

Fig.2: (a) Coverage of 16 lines of sight from two detector arrays (A and B) and typical flux surface contours. (b) and (c) The reconstructions of radiation distribution when plasma axis is located at $R = 702mm$ (dashed line) and $R = 720mm$ respectively. (d) Uncertainties of the reconstruction at R= 720mm for pulse #42602.

At TJ-II stellarator, the soft X-ray system consists of five cameras each having 16 detectors as shown in Fig.3(a). A comparison with reconstruction by the EBITA method [4] is in Fig.3(b).

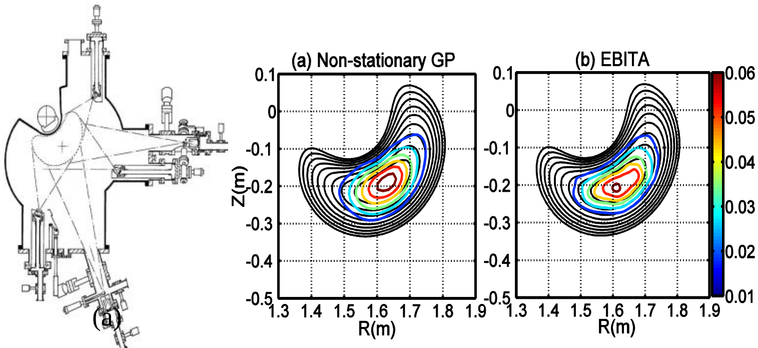

Fig.3: (a) Setup of a soft x-ray system. (b) Reconstructions by two methods.

4. Conclusion

The work aims to develop a new method for tomographic reconstructions of soft-x and bolometer data with unsymmetric and localized features. Through applications on different systems and comparisons with different inversion methods using both simulated and experimental data, convincing results have been achieved. Good agreements between this and other methods and also correspondence with equilibrium flux surfaces confirm this method further. Additionally, uncertainties of the results can be provided, taking into account both measurement uncertainty and line of sight coverage. Without any nonlinearity and numerical iteration, this calculation is also fast enough for real time applications.

References

[1]J. Svensson, Non-parametric tomography using Gaussian processes, JET pinboard

[2]D.Li, J.Svensson, et.al. Bayesian Soft X-Ray Tomography using Non-stationary Gaussian Processes in reviewing process, Rev. Sci. Ins.

[3]K. Ertl, W.Von der Linden, V. Dose and A. Weller, Nuclear Fusion **36**, 1477 (1996).

[4]A.P. Navarro, M.A. Ochando, and A. Weller, IEEE Tans. Plasma Sci. **19**, 569 (1991).

[5]C.E.Rasmussen, C.K.I. Williams, Gaussian Processes for Machine Learning, (MIT Press, 2006), p.79.

[6]N. Choudhuri, S. Ghosal and A. Roy, Statistical Methodology **4** (2007) 227–243.

[7] A. Weller, et al. Plasma Physics and Controlled Fusion **45** (2003) A285–A308.

[8]S.P. Hirshman, et al. Computer Physics Communications **43** (1986) 143-155, North-Holland, Amsterdam.